Acta Math. Univ. Comenianae
Vol. LXX, 1(2001), pp. 123–151
Proceedings of Algoritmy 2000

MATHEMATICAL AND COMPUTATIONAL ASPECTS OF SOLIDIFICATION OF PURE SUBSTANCES

M. BENEŠ

Abstract. The aim of the article is to deliver an information on the state of the art in the field of modelling of microstructure growth in a solidifying pure substance with a stress on the phase-field approach. We briefly summarize the physical background of the problem. The phase-field method is then explained and its variants are mentioned. Justification and theoretical results concerning the model equations are necessary for a quantitatively correct use of the model. We give some examples of qualitative computational studies and introduce the reader into quantitative comparison techniques used for verification of the model.

1. Introduction

Solidification is one of important first-order phase transitions within the context of metal processing ([**19**], [**28**] for the fundamental information about, [**35**] for modelling of). Here, the body with some macroscopic geometry undergoes a change from the liquid state to the solid one or vice versa. The process concerns whole body (casting) or his part only (welding, surface treatment). On the microscopic level, a small neighborhood of an arbitrary point in the liquid phase is chosen and the transient short-time process of the solid growth is investigated. It is necessary to distinguish between the solidification of a pure liquid, and the solidification of a mixture of liquids (alloy). Crystal growth from a pure liquid is important for the semiconductor processing, whereas solidification of mixtures creating alloys is important for whole mechanical engineering.

The term "pure substance" is an idealization which allows to neglect mass diffusion process. In the consequence, solidification is driven by the temperature evolution only. The microstructure growth starts either by a process called homogeneous nucleation, or on small impurities (heterogeneous sites). The nuclei form small grains growing into simple or complex shapes depending on heat conditions in their neighborhood. The growing grains interact and compete. The global thermal conditions (main direction of the heat flux) can influence the grain growth which forms a columnar structure. At the end of the process, the grains fill the bulk, where the different crystallographic orientation of grains can be preserved.

Received January 10, 2001.
2000 *Mathematics Subject Classification.* Primary 80A22, 82C26, 35A40.
Key words and phrases. Solidification, microstructure growth, Stefan problem, phase field.

Presence of an interface between grains can decrease the quality of produced material (e.g., thermomechanical properties). This is one of main reasons for the investigation of the microstructure formation.

In the phase transition theory, two streams can be distinguished. The Gibbs approach (more frequent) considers a sharp phase interface where a discontinuity of some system variables is assumed. One of consequences is the Stefan problem where the interface is defined by the melting temperature. To include the surface effects (surface tension, undercooling), the Stefan problem has been modified. In [**24**], models of phase transitions with interfacial energy and surface tension have been presented. A minimization of the bulk free energy under a mass constraint yields the desired solution. In case of a pure solidifying substance, the Gibbs-Thomson relation has been included into the Stefan problem but, unfortunately, there is a lack of a general theory here.

The other — van der Waals' — approach assumes a non-sharp but thin transition layer between phases where all the thermodynamical parameters vary continuously (see [**36**]). Ideas of van der Waals have been re-discovered by Cahn and Hilliard in 1950's (see [**17**], [**18**]) and the theory originally created for an explanation of the spinodal decomposition has been successfully applied in case of a pure solidifying substance ([**26**], [**29**]), as well as in case of an alloy ([**44**]).

In the literature, a competition between these two approaches can be observed during a century. The increasing computer power already allows to deal with complex microstructure phenomena. Especially here, the second approach shows up the advantage because it is easier to implement. The mentioned fact led the author to the application of the phase field approach for the simulation of the microstructure growth.

Classical Stefan problem. The phase transition process in a spatial domain is described by the Stefan problem known for more than 100 years.

$$\rho c \frac{\partial u}{\partial t} = \nabla \cdot (\lambda \nabla u) \text{ in } \Omega_s \text{ and } \Omega_l. \tag{1}$$

$$\lambda \frac{\partial u}{\partial n_\Gamma}\bigg|_s - \lambda \frac{\partial u}{\partial n_\Gamma}\bigg|_l = L v_\Gamma. \tag{2}$$

$$u\,|_\Gamma = u^*. \tag{3}$$

$$u\,|_{\partial\Omega} = u_\Omega. \tag{4}$$

$$u\,|_{t=0} = u_0, \qquad \Omega_s(t)\,|_{t=0} = \Omega_{so}. \tag{5}$$

We use the following notations:

- u, u^* temperature, melting point,
- L, ρ, c, λ material parameters,
- $\mathbf{n}_\Gamma$ outer normal to solid subdomain,
- v_Γ normal velocity of interface.

The presence of a free boundary Γ between the two phases makes the problem interesting and non-trivial from both mathematical and numerical viewpoints. As follows from the literature, the problem (1-4) and its variants were successfully treated (see [**43**] for an exhausting list of references).

Numerical solution of the Stefan problem is usually based on front tracking methods ([**42**]) where the free boundary is followed explicitly, or methods where the free boundary is implicitly involved in the algorithm and is obtained afterwards ([**13**], [**30**] and others).

As an example, we present here a simulation of a steel cylinder solidifying under axisymmetrical circumstances ([**11**]) — Figure 1. Here are main parameters of the simulation:

- steel cylinder diameter 30 cm, height 50 cm;
- steel percentage composition besides Fe is 0.3 C, 0.6 Mn, 0.3 Si, 0.03 P, 0.03 S, 0.15 Cr, 0.2 Ni;
- boundary average heat flux 10 W m^{-2}

The numerical algorithm is based on FDM and solves a regularized heat-conduction problem derived by the enthalpy method ([**2**]).

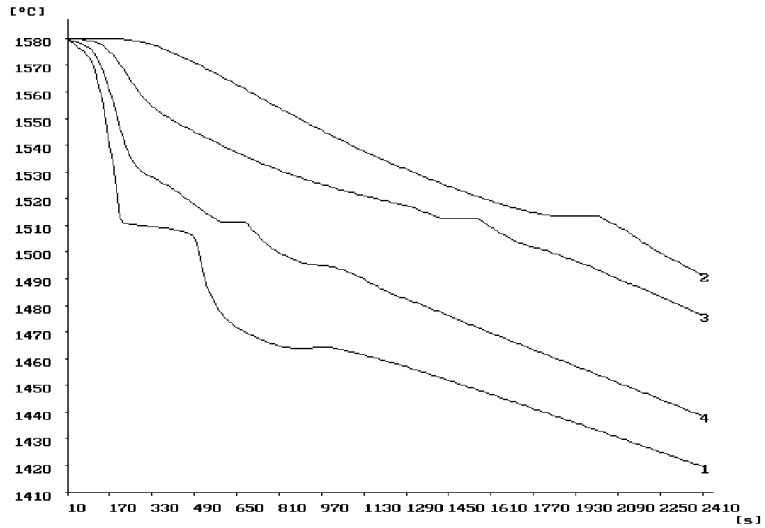

Figure 1. Temperature evolution at four positions in a solidifying cylinder under axisymmetrical conditions. Curves are denoted by numbers and have the following cylindrical coordinates r, z. [1]: $r = 0\text{cm}, z = 0\text{cm}$, [2]: $r = 8\text{cm}, z = 14\text{cm}$, [3]: $r = 2\text{cm}, z = 14\text{cm}$, [4]: $r = 8\text{cm}, z = 0\text{cm}$.

References for the Stefan problem. We refer the reader to the monograph [**43**] and a review [**41**] where an exhausting list of literature and historical remarks can be found.

2. Physical Models of Microstructure Growth

Constitutive relations describing phase transition phenomena on the microscopic level. The solidification of a pure material belongs to the class of first order phase transitions where the energy of self-organization is liberated

during the process. The Stefan problem for melting or freezing is obtained by evaluating the heat balance of the system. Formation of microstructure in the system is a result of changes in an other kind of energy, linked to the structural organization (free energy or entropy). Heat and free energy interact during the transient solidification process and can lead to the development of unstable complex shapes in the solid subdomain (e.g., cells, dendrites). If the system is achieving its equilibrium, these shapes are destroyed and the solid subdomain adopts an other, simpler form. A detailed analysis of the phase transition with more kinds of energy has been performed in [**24**], where thermodynamical relations leading to a model of solidification with interfacial energy and entropy have been derived. The theory confirms facts mentioned above and states that, in a bounded domain, no complex shapes are possible at the equilibrium.

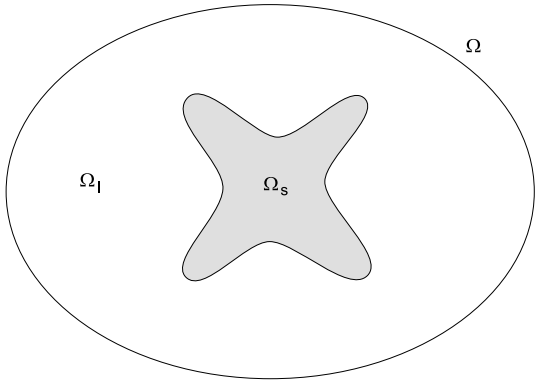

Figure 2. Domain Ω divided into the growing solid and vanishing liquid.

Be $\Omega \subset \mathbb{R}^2$ a bounded domain where the phase transition occurs, $\Omega_l(t)$, $\Omega_s(t)$ liquid and solid subdomain, respectively (see Figure 2), $\langle 0, T\rangle$ a time interval, $u\,\langle 0, T\rangle \times \bar{\Omega} \to \mathbb{R}$ the temperature field. Define the following relations:

- Constitutive equations of material (index s means solid, l liquid):

$H_s = H_s(u)$, $H_l = H_l(u)$	bulk enthalpy per unit volume;
$S_s = S_s(u)$, $S_l = S_l(u)$	bulk entropy per unit volume;
$F_s(u) = H_s(u) - uS_s(u)$,	
$F_l(u) = H_l(u) - uS_l(u)$	bulk free energy per unit volume.

- Constitutive equations for the interface $\Gamma(t) = \partial\Omega_s(t) \cap \partial\Omega_l(t)$:

$e = e(u)$	interfacial energy per unit area;
$s = s(u)$	interfacial entropy per unit area;
$f(u) = e(u) - us(u)$	interfacial free energy per unit area.

The latent heat per unit volume is defined as

$$L = H_l(u^*) - H_s(u^*),$$

where the transition temperature u^* is given as a temperature, where free energies are equal (Figure 3):

$$F_l(u^*) = F_s(u^*).$$

The complete system of field equations and free-boundary conditions for the general nonlinear theory is (see [**24**]):

$$\begin{aligned}
\frac{\partial H_s(u)}{\partial t} &= -\nabla \mathbf{q}_s \ , \quad \mathbf{q}_s = -\lambda_s(u)\nabla u \quad \text{in } \Omega_s(t), \\
\frac{\partial H_l(u)}{\partial t} &= -\nabla \mathbf{q}_l \ , \quad \mathbf{q}_l = -\lambda_l(u)\nabla u \quad \text{in } \Omega_l(t), \\
u &= \frac{H_l \mid_l - H_s \mid_s - \kappa_\Gamma e}{S_l \mid_l - S_s \mid_s - \kappa_\Gamma s} \quad \text{on } \Gamma(t), \\
(\mathbf{q}_l \mid_l - \mathbf{q}_s \mid_s) n_\Gamma &= v_\Gamma (H_l \mid_l - H_s \mid_s) - \kappa_\Gamma e v_\Gamma - D_t e \quad \text{on } \Gamma(t), \\
v_\Gamma n_\Gamma \cdot n_{\partial\Omega} &= 0 \quad \text{on } \partial\Omega \cap \partial\Gamma(t).
\end{aligned} \tag{6}$$

Here, the following symbols have been used:

λ_s, λ_l	heat conductivity;
$\kappa_\Gamma = \nabla \cdot \mathbf{n}_\Gamma$	mean curvature of the hypersurface $\Gamma(t)$;
$\mathbf{n}_\Gamma$	normal unit vector to $\Gamma(t)$ pointing out of Ω_s;
$\mathbf{n}_{\partial\Omega}$	normal unit vector to $\partial\Omega$ pointing out of Ω;
v_Γ	normal velocity of $\Gamma(t)$;
$\mathbf{q}$	heat flux;
$D_t e$	derivative of e with respect to time variable at $\Gamma(t)$.

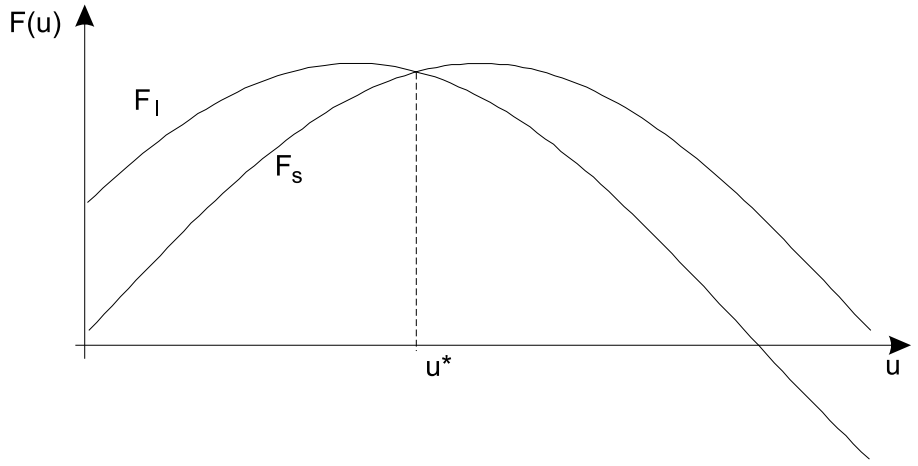

Figure 3. Free energies of solid (F_s) and liquid (F_l) phase as functions of temperature u define melting point u^*.

In the rest, the constitutive hypothesis is supposed to be valid:

1. Definition of enthalpy
$$H_s(u) = \int_0^u \rho_s(u)c_s(u)\,du,$$
$$H_l(u) = \int_0^u \rho_l(u)c_l(u)\,du + L,$$
with $\rho(u), c(u)$ material characteristics (density, heat capacity);
2. Difference in entropy per unit volume
$$S_l\,|_l - S_s\,|_s = \Delta s.$$
3. Intersection of boundary and interface
$$\partial\Gamma(t) \cap \partial\Omega = \emptyset \quad \forall t \geq 0.$$
4. Scaling
$$\frac{su^*}{L} \ll 1.$$
5. Presence of kinetic undercooling modifying the temperature relation at $\Gamma(t)$.

Under these assumptions, the general system (6) can be simplified into the form:

$$\rho c\frac{\partial u}{\partial t} = \nabla(\lambda\nabla u) \quad \text{in } \Omega_s \text{ and } \Omega_l,$$

$$b_c(u)\,|_{\partial\Omega} = 0, \tag{7}$$

$$u\,|_{t=0} = u_0, \tag{8}$$

$$\lambda\frac{\partial u}{\partial n}\bigg|_s - \lambda\frac{\partial u}{\partial n}\bigg|_l = Lv_\Gamma, \tag{9}$$

$$u - u^* = -\frac{\sigma}{\Delta s}\kappa_\Gamma - \alpha\frac{\sigma}{\Delta s}v_\Gamma, \tag{10}$$

$$\Omega_s(t)\,|_{t=0} = \Omega_{so}. \tag{11}$$

Discontinuity of heat flux on $\Gamma(t)$ is described by the Stefan condition (9), the formula (10) is the Gibbs-Thomson relation on $\Gamma(t)$, where $\sigma = f(u^*)$ is the surface tension between the two phases, and α is the coefficient of attachment kinetics. The boundary condition (7) is expressed by the operator b_c in one of the following forms:

- Dirichlet boundary condition
$$b_c(u) = u - u_{\partial\Omega}.$$
- Neumann boundary condition with the heat flux $\mathbf{g}$ on $\partial\Omega$
$$b_c(u) = (\lambda(u)\nabla u - \mathbf{g}) \cdot \mathbf{n}_\Gamma.$$

The conditions (8) and (11) are the initial conditions for temperature, and spatial distribution of the solid and liquid phase.

Simulation techniques. Models of microstructure formation can be based on various techniques. We can classify first group of them as **two-domain** methods,

or front tracking (using either BEM [**37**], FEM [**38**] or other variational methods [**1**]) because the free boundary is explicitly treated by the algorithm. The **single-domain** or implicit methods do not explicitly treat the interface which is usually obtained afterwards (FDM based levelset methods of [**39**], FEM based methods, e.g. [**21**]). The phase-field method is subject of this article. Last group of **particle** methods contains DLA algorithms [**22**], Monte Carlo simulations [**45**], or cellular automata [**15**].

3. Phase-field Theory

In this section, we present constitutive relations describing the phase transition between liquid and solid, the phase field theory and the formulation of the phase-field model for solidification of a pure substance. The model is then analysed from point of view of thermodynamics, differential geometry and dimensionality. Finally, the mechanism of the formal matched asymptotics is used to recover sharp-interface relations.

Practical reasons (difficulties with the interface tracing) and increasing power of computers led to another attempts of description of a first-order phase transition. One of them has the origin in the van der Waals theory [**36**]. It is based on a non-sharp interpretation of the phase interface, which was presented by Cahn and Hilliard in the context of phase separation (see [**17**], [**18**]). Here, the non-convex functional of the bulk free energy has been expressed by the volumic density depending on the value in a neighborhood of any point (using Taylor expansion).

Denote dimension of the the domain Ω of interest as $n = \dim \Omega$. Let $\mathcal{F}$ be a thermodynamic functional (e.g., of free energy), expressed using its volumic density which depends on a set of order parameters $\{p_1, \dots, p_m\}$. Following [**17**], [**18**], we assume that the functional $\mathcal{F}$ has the form

$$\mathcal{F}[p_1, \dots, p_m] = \int_\Omega \left(w(p_1, \dots, p_m) + T(Dp_1, \cdots, Dp_m)\right) dx. \tag{12}$$

The expression consists of the bulk density w and a gradient term T which describes a non-uniformity of the system. Usually, the function w is of "multi-well" type so that the system will prefer certain states given by special values of order parameters $\{p_1, \dots, p_m\}$ (see [**25**], [**44**]). If the system evolves in time, the functional relaxes towards the minimum value in a non-oscillatory way (see [**23**]) described by the so-called Model A equation [**25**]

$$\tau_i \frac{\partial p_i}{\partial t} = -\delta_{p_i} \mathcal{F}[p_1, \dots, p_m] \,, \quad i = 1, \dots, m, \tag{13}$$

where $\delta_{p_i}\mathcal{F}$ is the Frchet derivative of $\mathcal{F}$ and τ_i is a relaxation parameter.

Let the system state be described by a parameter p ($m = 1$), and let its behaviour be driven by a field $u = u(t, x)$ (e.g., temperature distribution in the bulk). It is expected that p is near 0, if the system is locally in the liquid state, near 1, if it is locally in the solid state. The transition from one to another state should take place in a thin transition layer (see Figure 4), and superheating (supercooling) phenomena should be allowed. Such requirements are satisfied by w in the

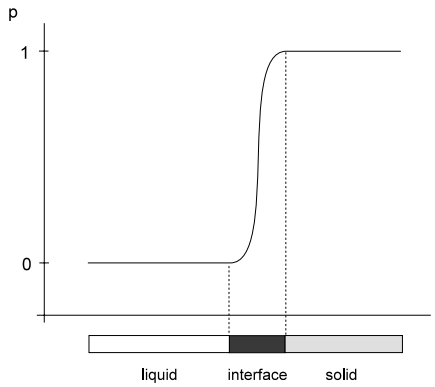

Figure 4. Phase function as an approximation of the indicator function of solid.

form of double-well potential (Figure 5), and by the presence of a small parameter $\xi > 0$ in the functional $\mathcal{F}$, which is related to the transition-layer thickness.

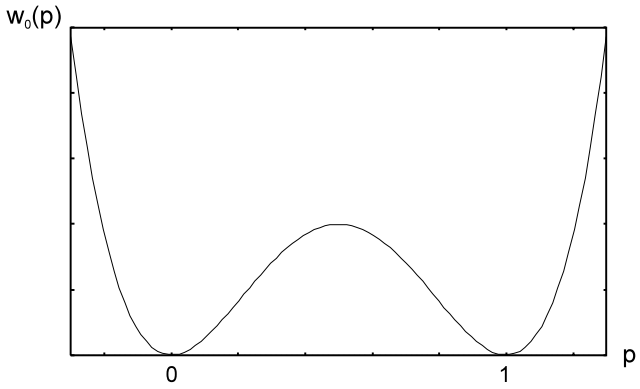

Figure 5. Double-well potential with two minima at stable states 0 and 1.

Consider functionals

$$\mathcal{H}[p,u] = \int_0^u \rho(u',p)c(u',p)\,du' + L(1-p),$$

$$\mathcal{F}[p,u] = \int_\Omega \left(w_0(p,u;\xi) + T(\nabla p;\xi)\right)\,dx, \tag{14}$$

where ρ, c, λ are material characteristics, L is the latent heat per unit volume. The fields evolve according to the equations

$$\frac{\partial \mathcal{H}[u,p]}{\partial t} = \nabla\left(\lambda(u)\nabla u\right), \tag{15}$$

$$\tau\frac{\partial p}{\partial t} = -\delta_p \mathcal{F}[p,u]. \tag{16}$$

The first one is heat equation, and the second one is called phase equation. We calculate the variation of $\mathcal{F}$ with respect to the variation δp of the phase function p:

$$\begin{aligned}
&\mathcal{F}[p+\delta p,u;\xi]\\
&=\int_\Omega\left(w(p,u;\xi)+\frac{\partial w(p,u;\xi)}{\partial p}\delta p+T(\nabla p;\xi)+\sum_{j=1}^n\frac{\partial T(\nabla p;\xi)}{\partial g_j}\frac{\partial\delta p}{\partial x_j}+\dots\right)dx\\
&=\int_\Omega\left(w(p,u;\xi)+T(\nabla p;\xi)+\frac{\partial w(p,u;\xi)}{\partial p}\delta p-\sum_{j=1,k=1}^n\frac{\partial^2T(\nabla p;\xi)}{\partial g_j\partial g_k}\frac{\partial^2p}{\partial x_j\partial x_k}\delta p+\dots\right)dx\\
&\quad+\int_{\partial\Omega}\sum_{j=1}^n\frac{\partial T(\nabla p;\xi)}{\partial g_j}\delta p\ n_{\Gamma j}\,dS,
\end{aligned}$$

where $T=T(g_1,\dots,g_n;\xi)$, and $g_1,\dots,g_n$ denote components of ∇p.

The boundary integral vanishes if

$$\delta p|_{\partial\Omega}=0,$$

or

$$\left.\frac{\partial T(\nabla p;\xi)}{\partial\mathbf{n}_{\partial\Omega}}\right|_{\partial\Omega}=0.$$

Consequently, the Fréchet derivative of $\mathcal{F}$ with respect to p is

$$\delta_p\mathcal{F}[p,u;\xi]=-\sum_{j=1,k=1}^n\frac{\partial^2T(\nabla p;\xi)}{\partial g_j\partial g_k}\frac{\partial^2p}{\partial x_j\partial x_k}+\frac{\partial w(p,u;\xi)}{\partial p}.$$

The resulting system of field equations is

$$\rho(u)c(u)\frac{\partial u}{\partial t}=\nabla\left(\lambda(u)\nabla u\right)+L\frac{\partial p}{\partial t},\tag{17}$$

$$\tau(\xi)\frac{\partial p}{\partial t}=\sum_{i,j=1}^n\frac{\partial^2T(\nabla p;\xi)}{\partial g_i\partial g_j}\frac{\partial^2p}{\partial x_i\partial x_j}-\frac{\partial w(u,p;\xi)}{\partial p}.\tag{18}$$

The boundary conditions admissible for the boundary value problem related to the Fréchet derivative are given by the conditions above

- Dirichlet

$$u|_{\partial\Omega}=u_\Omega,\quad p|_{\partial\Omega}=p_\Omega;\tag{19}$$

- Neumann

$$\left.\frac{\partial u}{\partial\mathbf{n}_{\partial\Omega}}\right|_{\partial\Omega}=0,\quad\left.\frac{\partial T(\nabla p;\xi)}{\partial\mathbf{n}_{\partial\Omega}}\right|_{\partial\Omega}=0.\tag{20}$$

The system of equations (17) and (18) completed by appropriate boundary (19) or (20) and initial conditions form the system of phase-field equations.

4. Various Forms of the Phase Equation

The phase equation exhibits a singular behaviour caused by the interaction of a small diffusion coefficient — usually,

$$\frac{\partial^2 T(\nabla p;\xi)}{\partial g_i \partial g_j} \approx \xi^2 \delta ij,$$

within the differential operator, and of the double-well potential. This fact led to the idea that it is possible to recover mean-curvature flow in the physical context of the Stefan problem or of the modified Stefan problem, if using a special limiting procedure.

Consider the Gibbs — Thomson relation between interface velocity v_Γ, mean curvature κ_Γ, and the undercooling of the interface $\Delta u = u - u^*$

$$\Delta s \Delta u = -\sigma\kappa_\Gamma - \alpha\sigma v_\Gamma, \tag{21}$$

where Δs is difference in entropy density, σ surface tension, α attachment-kinetics coefficient. Then, the relaxation-time parameter τ adopts the form of

$$\tau(\xi) = \alpha\xi^2,$$

which is justified by the asymptotical analysis of the model with respect to $\xi \to 0$.

Isotropic form of the gradient term in (14) is

$$T(\nabla p;\xi) = \xi^2 |\nabla p|_E^2.$$

where $|\cdot|_E$ denotes the Euclidean norm.

Model 1. The right-hand-side function $f = \frac{\partial w}{\partial p}$ is subject of further modifications. The original form proposed in [**16**] was

$$f(p,u;\xi) = ap(1-p)(p-0.5) - b\beta\xi(u-u^*), \tag{22}$$

where a, b, $\beta = \frac{\Delta s}{\sigma}$ are positive constants. The advantage is in the linear dependence on the driving parameter (temperature) u. However, for certain values of β and ξ, it looses the desirable behaviour in the following sense (see Figure 6). The function f has three zeros, only if

$$b\beta\xi(u-u^*) \in \Big(-\frac{\sqrt{3}}{36}a, +\frac{\sqrt{3}}{36}a\Big).$$

If this condition is not satisfied, the solution of the phase-field equations has no more physical meaning (see [**6**]).

Model 2. Another form of the function f was proposed in [**27**]

$$f(p,u;\xi) = ap(1-p)(p-0.5-M(u-u^*;\xi)), \tag{23}$$

where

$$M(u;\xi) = b\xi \arctan(\gamma_0(u-u^*)), \quad \gamma_0 > 0,$$

is the coupling term containing the driving parameter u. Many computational studies have been performed using this form of f — see [**3**], [**4**], [**27**]. Due to the non-linearity of M, the Model 2 does not allow to recover the Gibbs-Thomson relation in the form (21).

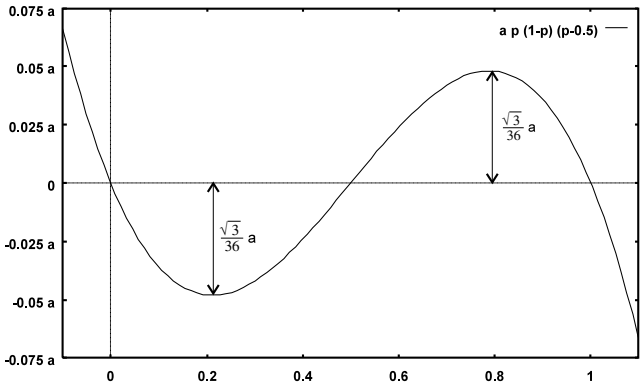

Figure 6. Derivative of double-well potential with two local extrema limiting correct behaviour of the Model 1.

Model 3. Attempts to improve behaviour of the phase equation led to the following form of function f (see [**5**], [**6**]).

$$f(p, \nabla p, u; \xi) = ap(1-p)(p-0.5) - \beta\xi^2 |\nabla p|_E (u - u^*). \tag{24}$$

It does not have disadvantages of the previous two cases. Such a gradient modification of the reaction term in the equation (18) is motivated by the related level-set formulation of the condition (21), and is less related to a thermodynamical functional of the form of (14) — for details, see Section 6. It is discussed in next chapters.

The previous definitions contain a physical parameter $\beta = \frac{\Delta s}{\sigma}$, and parameters a, b which must be determined by the mathematical analysis of the phase equation — see Section 7.

It also is possible to consider an **anisotropic Gibbs-Thomson condition** in the form of

$$\alpha v_\Gamma = -g(\theta)\kappa_\Gamma - \beta(u - u^*),$$

where g is a bounded

$$0 < g_1 \leq g(\theta) \leq g_2,$$

and positive function of the direction θ (angle between the outer normal to Ω_s and the axis x^1). Such a function g describes a non-faceted crystalline anisotropy. In this case, the corresponding phase equation is proposed in the form

$$\alpha\xi^2 \partial_t p = g(\theta)\Big[\xi^2 \nabla^2 p + ap(1-p)(p - \frac{1}{2})\Big] - \beta(u - u^*)\xi^2 |\nabla p|_E,$$

and, usually,

$$g(\theta) = 1 - \zeta \cos(n_{\text{fold}}\theta)$$

with $\zeta \in< 0, 1)$ being the n_{fold}-anisotropy strength. Compared to the Gibbs-Thomson relation which is valid at the interface, the phase equation requires prescription of appropriate boundary conditions. If it is known that the phase at the

boundary $\partial\Omega$ does not change (contact with the mould, directional solidification), the Dirichlet boundary condition is prescribed

$$p|_{\partial\Omega} = p_\Omega.$$

If the model should describe the situation in a cell inside of melt, where the pattern grows from the liquid undercooled below the melting point, the homogeneous Neumann condition can be used

$$\left.\frac{\partial p}{\partial \mathbf{n}_\Omega}\right|_{\partial\Omega} = 0.$$

The driving parameter — u — is obtained from the heat-conduction equation

$$\rho(u)c(u)\frac{\partial u}{\partial t} = \nabla\left(\lambda(u)\nabla u\right) + L\frac{\partial p}{\partial t}. \tag{25}$$

Usually, the material parameters are constant, as the microstructure growth is stimulated by relatively small variations in temperature, where the material parameters vary negligibly. Boundary conditions correspond to those of the phase equation — the Dirichlet one in case of directional growth

$$u|_{\partial\Omega} = u_\Omega,$$

and the Neumann one in case of an adiabatically isolated domain in the melt.

$$\left.\frac{\partial p}{\partial \mathbf{n}_\Omega}\right|_{\partial\Omega} = 0.$$

In this work, the phase field model consisting of equations (25) and (18) is compared to the sharp-interface standard in order to figure out the behaviour and properties of the model. The following criteria are used:

- agreement of values v_Γ, κ_Γ, $u - u^*$ at Γ with the Gibbs-Thomson relation;
- small variation in the solution u and p far from Γ if $\xi \to 0$;
- CPU time (the best agreement under the easiest conditions imposed to the mesh size and time step used in the numerical solution);
- agreement in stability of sharp and diffusive (phase-field defined) interface.

As a **sharp-interface standard**, the modified Stefan problem (Stefan problem with surface tension, see [**24**]) has been chosen.

$$\rho c\frac{\partial u}{\partial t} = \nabla(\lambda\nabla u) \text{ in } \Omega_s \text{ and } \Omega_l, \tag{26}$$

$$b_c(u)\,|_{\partial\Omega} = 0 \text{ in } (0,T), \quad u\,|_{t=0} = u_0 \text{ in } \Omega,$$

$$\lambda\frac{\partial u}{\partial n}\,|_s - \lambda\frac{\partial u}{\partial n}\,|_l = L v_\Gamma \text{ on } \Gamma,$$

$$u - u^* = -\frac{\sigma}{\Delta s}\kappa_\Gamma - \alpha\frac{\sigma}{\Delta s}v_\Gamma \text{ on } \Gamma, \tag{27}$$

$$\Omega_s(t)\,|_{t=0} = \Omega_{so}. \tag{28}$$

It is worth mentioning, that the above criteria can be satisfied by using different coupling terms (see (22), (23), (24)).

Real scales. As a remark, we deliver an example of parameter values in Table 1, so that the reader can be aware of difference between the original physical setting and a dimensionless model.

$$\begin{aligned}
[u, \Delta u_{in}, u^*] &= \mathrm{K},\\
[L] &= \mathrm{J\ m^{-3}},\\
[\rho] &= \mathrm{kg\ m^{-3}},\\
[c] &= \mathrm{J\ kg^{-1}K^{-1}},\\
[\Delta s] &= \mathrm{J\ m^{-3}K^{-1}},\\
[\sigma] &= \mathrm{J\ m^{-2}},\\
[\alpha] &= \mathrm{s\ m^{-2}},\\
[\beta] &= \mathrm{m^{-1}K^{-1}},\\
[a] &= 1,\\
[b] &= 1,\\
[\xi] &= \mathrm{m},\\
[p] &= 1.
\end{aligned}$$

Real parameter	Value	Model parameter	Value
u^*	933.6 K	U^*	1.0
L_0	0.001 m	length scale	1.0
t_0	36.428 s	time scale	1.0
ρ	$2.55 \cdot 10^3$ kgm^{-3}	-	1.0
c	1176.47 $Jkg^{-1}K^{-1}$	-	1.0
λ	210 $Wm^{-1}K^{-1}$	-	1.0
Δu_{in}	0.124 K	$1 - U(0)$	1.0
L	$9.5 \cdot 10^8$ Jm^{-3}	K	1.0
Δs	$1.02 \cdot 10^6$ $Jm^{-3}K^{-1}$	-	-
σ	$93 \cdot 10^{-3}$ Jm^{-2}	-	-
β	$1.097 \cdot 10^7$ $m^{-1}K^{-1}$	β'	1360.28
μ	4.325 $mK^{-1}s^{-1}$	-	-
α	$2.536 \cdot 10^6$ $m^{-1}s$	α'	0.069

Table 1. Table of parameters for pure aluminium.

5. Justification for the Phase Equation by Thermodynamics

Compared to the original treatment of the phase-field model, where the functional of interest was free energy composed of a bulk and an interface terms, a more adequate procedure of how the phase equation arises from the physical context is

based on an entropic formulation (see [**34**], [**44**]). Let the system under consideration be described by two state variables — enthalpy H and order parameter p (phase function, or concentration of phase). Let the system entropy have the form

$$\mathcal{S}_\xi[H,p] = \int_\Omega \left(\frac{1}{\xi} s_0(H,p) - s_\Gamma \xi |\nabla p|_E^2 \right) dx,$$

where s_0 is bulk entropy density, and $s_\Gamma > 0$ is interface entropy density, $\xi > 0$ is a small parameter related to the interface-layer thickness. Evaluating the time derivative of $\mathcal{S}$ and using the Green formula, we obtain the following relation:

$$\begin{aligned} \dot{\mathcal{S}} &= \int_\Omega \left(\frac{1}{\xi} \frac{\partial s_0}{\partial H}(H,p) \frac{\partial H}{\partial t} + \frac{1}{\xi} \frac{\partial s_0}{\partial p}(H,p) \frac{\partial p}{\partial t} - 2\xi s_\Gamma \nabla p \cdot \nabla \Big(\frac{\partial p}{\partial t} \Big) \right) dx \\ &= \int_\Omega \left(\frac{1}{\xi} \frac{\partial s_0}{\partial H}(H,p) \frac{\partial H}{\partial t} + \frac{1}{\xi} \frac{\partial s_0}{\partial p}(H,p) \frac{\partial p}{\partial t} + 2\xi s_\Gamma \nabla^2 p \frac{\partial p}{\partial t} \right) dx \\ &\quad - 2\xi \int_{\partial\Omega} s_\Gamma \frac{\partial p}{\partial t} \nabla p \cdot \mathbf{n}_{\partial\Omega} \, dS \end{aligned} \tag{29}$$

According to the enthalpy conservation law in case of zero bulk sources

$$\frac{\partial H}{\partial t} = -\nabla \mathbf{q},$$

where $\mathbf{q}$ is heat flux, we have

$$\begin{aligned} \dot{\mathcal{S}} = \int_\Omega \left(\frac{1}{\xi} \nabla \Big(\frac{\partial s_0}{\partial H}(H,p) \Big) \cdot \mathbf{q} + \frac{1}{\xi} \frac{\partial s_0}{\partial p}(H,p) \frac{\partial p}{\partial t} + 2\xi s_\Gamma \nabla^2 p \frac{\partial p}{\partial t} \right) dx \\ - \int_{\partial\Omega} \frac{1}{\xi} \frac{\partial s_0}{\partial H}(H,p) \mathbf{q} \cdot \mathbf{n}_{\partial\Omega} \, dS - 2\xi \int_{\partial\Omega} s_\Gamma \frac{\partial p}{\partial t} \nabla p \cdot \mathbf{n}_{\partial\Omega} \, dS. \end{aligned}$$

The volumic integral in the previous expression is called entropy production

$$\mathcal{P} = \int_\Omega \left(\frac{1}{\xi} \nabla \Big(\frac{\partial s_0}{\partial H}(H,p) \Big) \cdot \mathbf{q} + \frac{1}{\xi} \frac{\partial s_0}{\partial p}(H,p) \frac{\partial p}{\partial t} + 2\xi s_\Gamma \nabla^2 p \frac{\partial p}{\partial t} \right) dx, \tag{30}$$

and according to [**33**], it is non-negative (second law of thermodynamics)

$$\mathcal{P} \geq 0.$$

Such a condition is satisfied, if

$$\begin{aligned} \mathbf{q} &= \lambda \nabla \Big(\frac{\partial s_0}{\partial H} \Big), \quad \lambda > 0, \\ \tau \xi \frac{\partial p}{\partial t} &= \frac{1}{\xi} \frac{\partial s_0}{\partial p}(H,p) + 2\xi s_\Gamma \xi p, \quad \tau > 0. \end{aligned}$$

The first of the previous relations is the well-known Fourier law for heat flux and the second relation is the phase equation, which is in agreement with the principle of minimum entropy production, in addition (see [**33**]). The above analysis represents a non-sharp approach to phase transitions, whose origin can be found in [**36**]. The functional $\mathcal{S}$ is, in fact, an approximation of a thermodynamic functional, if $\xi \to 0$. The above mentioned implications indicate a deep connection of the phase equation and of the out-of-equilibrium thermodynamics of the problem.

6. Justification of the Phase Equation by Differential Geometry

Consider the Gibbs-Thomson relation

$$u - u^* = -\frac{\sigma}{\Delta s}\kappa_\Gamma - \alpha\frac{\sigma}{\Delta s}v_\Gamma.$$

Let the interface Γ be described by a mapping $\Phi : \mathbb{R}^n \to \mathbb{R}$ as follows

$$\Gamma = \{x \in \mathbb{R}^n \mid \Phi(x) = 0\},\ \Omega_s = \{\Phi(x) > 0\},$$

that is, the interface Γ is the 0-level set of the mapping Φ. In addition, let the mapping Φ depends on time. Then Γ also depends on time. If Φ is smooth enough and $\nabla\Phi$ is non-zero along Γ, it can be used to express the outer normal and normal interface velocity

$$\mathbf{n}_\Gamma = -\frac{\nabla\Phi}{|\nabla\Phi|_E} \quad , \quad v_\Gamma = \frac{\frac{\partial\Phi}{\partial t}}{|\nabla\Phi|_E}.$$

Similarly, mean curvature is expressed as

$$\kappa_\Gamma = \nabla\cdot\mathbf{n}_\Gamma = -\nabla\cdot\Big(\frac{\nabla\Phi}{|\nabla\Phi|_E}\Big)|_\Gamma\,.$$

Substituting the previous expressions into (27), we obtain

$$\Delta s(u-u^*) = \sigma\nabla\cdot(\frac{\nabla\Phi}{|\nabla\Phi|_E}) - \alpha\sigma\frac{\frac{\partial\Phi}{\partial t}}{|\nabla\Phi|_E}.$$

Assuming validity of the previous equation on whole Ω (increasing dimension of the problem), the level-set formulation of the Gibbs-Thomson equation is obtained. Still one form of the level-set formulation is used

$$\alpha\sigma\frac{\partial\Phi}{\partial t} = \sigma|\nabla\Phi|_E\nabla\cdot\Big(\frac{\nabla\Phi}{|\nabla\Phi|_E}\Big) + \Delta s|\nabla\Phi|_E(u^*-u). \tag{31}$$

The origin of (24) can be found in the last term of the previous equations. Solving the equation (31) means solving the Riemann problem ([**40**]) on Ω. For the analysis of it, see [**20**]. The phase equation is a regularization of (31) in certain sense. In addition, it has an advantage compared to (31). The function p typically has a profile of Figure 4, so that the phase equation has non-trivial sense in a thin sublayer Ω_Γ only (2.5-dimensional problem).

7. Theoretical Background

We may review some theoretical results obtained especially for the phase-field model based on the **Model** 3. setting with the gradient coupling term:

$$\begin{aligned}\frac{\partial u}{\partial t} &= \nabla^2 u + L\frac{\partial p}{\partial t},\\ \alpha\xi^2\frac{\partial p}{\partial t} &= \xi^2\nabla^2 p + ap(1-p)(p-0.5) + F(u)\xi^2|\nabla p|_E,\end{aligned} \tag{32}$$

where F is a bounded Lipschitz-countinuous function of temperature describing the undercooling. The following notations are used:

$$|\mathbf{z}|_E = \sqrt{|z^1|^2 + |z^2|^2} \text{ for } \mathbf{z} = [z^1, z^2] \in \mathbb{R}^2,$$

$$(\!(u,v)\!) = \int_\Omega \nabla u \cdot \nabla v \; dx \text{ for } u, v \in \mathrm{H}^1(\Omega),$$

$$\|u\| = \sqrt{\int_\Omega u(x)^2 dx} \text{ for } u \in \mathrm{L}_2(\Omega),$$

$$w_0(p) = -f_0(p), \quad f_0(p) = ap(1-p)\left(p - \frac{1}{2}\right),$$

The equations (32) represent a reaction-diffusion system with a polynomial non-linearity in p and transcendent non-linearity in ∇p. Following [**9**], we define the notion of the weak solution as usual in:

Definition 1. Weak solution of the boundary-value problem with homogeneous Dirichlet boundary conditions for the phase-field equations is a couple of functions $[u,p]$ from $(0,T)$ to $[\mathrm{H}_0^1(\Omega)]^2$, each in $\mathrm{L}_2(0,T,\mathrm{H}_0^1(\Omega))$ such that it satisfies

$$\begin{aligned} \frac{d}{dt}(u,v) + (\!(u,v)\!) &= L\frac{d}{dt}(p,v) \text{ a.e. in } (0,T), \\ u(0) &= u_0, \\ \alpha\xi^2\frac{d}{dt}(p,q) + \xi^2(\!(p,q)\!) &= (f_0(p),q) + \xi^2(F(u)|\nabla p|_E, q) \text{ a.e. in } (0,T), \\ p(0) &= p_0. \end{aligned} \tag{33}$$

for each $v, q \in \mathrm{H}_0^1(\Omega)$.

The existence and uniqueness result is contained in the following theorem proved in [**9**]:

Theorem 1. *Consider the problem* (33) *in a bounded domain with Lipschitz-continous boundary* $\Omega \subset \mathbb{R}^2$ *with*

$$u_0, p_0 \in \mathrm{H}_0^1(\Omega). \tag{34}$$

F be a bounded Lipschitz-continuous function. Then, there is a unique solution of the problem (33) *satisfying*

$$u, p \in \mathrm{L}_\infty(0,T;\mathrm{H}_0^1(\Omega)), \;\; p \in \mathrm{L}_2(0,T;\mathrm{H}^2(\Omega)),$$

$$\partial_t u, \partial_t p \in \mathrm{L}_2(0,T;\mathrm{L}_2(\Omega)).$$

Remark. The relationship of the phase-field equations to the sharp-interface formulation is demonstrated by matched asymptotical analysis [**6**], [**10**]. We are interested in recovering the sharp-interface relations. The equations (32) have a solution in the form

$$u = u(t,x;\xi),\; p = p(t,x;\xi).$$

Due to a special form of the phase equation composed of a very small diffusion term and of derivative of a double-well function, it is expected that a thin layer Ω_Γ between two major domains — phases appear, where the function p quickly changes its value (see [**6**]).

There is a statement which confirms that the field p tends to a step-wise function as expected (see [**6**] and [**14**]). More precisely, a priori estimates of the weak solution imply that the energy functional

$$E_\xi[p](t) = \int_\Omega \left[\xi \frac{1}{2} |\nabla p|_E^2 + \frac{1}{\xi} w_0(p) \right] dx,$$

is bounded as

$$E_\xi[p](t) \le E_\xi[p](0) \exp\left\{ \frac{C_F^2}{2\alpha} t \right\} \quad t \in (0,T),$$

where p is second component of the solution of (33). From [**6**], there is an estimate for the time derivative by

$$\frac{1}{2}\alpha\xi \int_0^T \|\partial_t p\|^2 \, dt + E_\xi[p](T) \le C_T E_\xi[p](0).$$

This allows to state the following theorem (proved in [**12**, Section 2.3].):

Theorem 2. *Let $[u,p]$ ($u = u(t,x;\xi)$, $p = p(t,x;\xi)$) is the solution of* (33) *with the initial data satisfying $E_\xi[p](0) < M_0$ independently on ξ, and let*

$$\int_\Omega |p(0,x;\xi) - v_0(x)| \, dx \to 0,$$

as $\xi \to 0$, for a function $v_0 \in \mathrm{L}_1(\Omega)$. Then for any sequence ξ_n tending to 0 there is a subsequence $\xi_{n'}$ such that

$$\lim_{\xi_{n'} \to 0} p(t,x;\xi_{n'}) = v(t,x),$$

is defined a.e. in $(0,T) \times \Omega$. The function v reaches values 0 and 1, and satisfies

$$\int_\Omega |v(t_1,x) - v(t_2,x)| \, dx \le C |t_2 - t_1|^{\frac{1}{2}},$$

where $C > 0$ is a constant, and

$$\sup_{t \in \langle 0,T \rangle} \int_\Omega |\nabla v|_E \, dx \le C_1,$$

in the sense of $BV(\Omega)$, where $C_1 > 0$ is a constant. The initial condition is

$$\lim_{t \to 0_+} v(t,x) = v_0(x),$$

a.e.

The information about a relation valid on the interface Γ comes from the formal asymptotical analysis with respect to the "small" parameter ξ applied to (32) (for details, see [**10**]). All quantities in the model are expanded far from the interface; e.g. for the solution, we assume

$$u(t,\mathbf{x};\xi) = u_0(t,\mathbf{x}) + u_1(t,\mathbf{x})\xi + u_2(t,\mathbf{x})\xi^2 + \mathcal{O}(\xi^3),$$
$$p(t,\mathbf{x};\xi) = p_0(t,\mathbf{x}) + p_1(t,\mathbf{x})\xi + p_2(t,\mathbf{x})\xi^2 + \mathcal{O}(\xi^3),$$

and near the interface, where a radial-tangential coordinate system (z, s) is used

$$\bar{u}(z,s,t;\xi) = \bar{u}_0(z,s,t) + \bar{u}_1(z,s,t)\xi + \bar{u}_2(z,s,t)\xi^2 + \mathcal{O}(\xi^3),$$
$$\bar{p}(z,s,t;\xi) = \bar{p}_0(z,s,t) + \bar{p}_1(z,s,t)\xi + \bar{p}_2(z,s,t)\xi^2 + \mathcal{O}(\xi^3).$$

Then, we obtain a result proved in [**10**, Theorem 4.5]

Theorem 3. *On the manifold Γ_0, the Stefan condition for the absolute terms in the outer expansion of temperature holds:*

$$\frac{\partial u_0}{\partial r}\Big|_s - \frac{\partial u_0}{\partial r}\Big|_l = L v_{\Gamma,0},$$

and the Gibbs Thomson law for the absolute term in the inner expansion of the phase function holds:

$$\int_{\mathbb{R}} \left(-\kappa_{\Gamma,0}\frac{\partial \bar{p}_0}{\partial z} - F(\bar{u}_0)\left|\frac{\partial \bar{p}_0}{\partial z}\right| - \alpha \frac{\partial \bar{p}_0}{\partial z} v_{\Gamma,0} \right) \frac{\partial \bar{p}_0}{\partial z}\, dz = 0.$$

The order of accuracy is treated by the statement proved in [**10**, Lemma 4.6]

Lemma 1. *The Gibbs-Thomson law on Γ_0 is satisfied up to the order 2 in terms of formal asymptotic expansion:*

$$F(\bar{u}_0) = \kappa_{\Gamma,0} + \alpha v_{\Gamma,0},$$
$$\alpha v_{\Gamma,1} + \kappa_{\Gamma,1} - F'(\bar{u}_0)\bar{u}_1 = 0.$$

Remark. The above mentioned results concern the isotropic modified phase-field model (32). The model has been further improved concerning the release of latent heat in [**10**]. The anisotropic version of the model has been derived by means of Finsler geometry in [**8**].

8. Computational Studies by the Phase-Field Model

The model discussed above allows to simulate microscopic phenomena arising in the solidification of a pure material. Appearance of complex patterns is a consequence of interface undercooling, surface tension, attachment kinetics and temperature gradient. Many numerical studies have been performed in order to study behaviour of the model, its qualitative and quantitative agreement with reality and other models of phenomena in question. The selected results should give sufficient information about it. The Tables 2 and 3 summarize sense and relation of real and model parameters.

Each figure is a graphical representation of the state of the system at a defined moment of time. Left, there is the temperature field with values represented by a shadowed scale of isotherms. The phase field (characteristic function of the solid subdomain $\Omega_s(t)$) is visualized using a different scale of isovalues (right). Numerical scheme consists of FDM discretization in space and of Runge-Kutta Method in time. The standard algorithm of the method of lines can be modified by the double-grid option (the grid for the heat conduction equation can be twice sparser than the grid for the phase field equation).

Real parameter	Sense
u^*	melting point
t_0	time scale
$L_0 = \sqrt{\frac{\lambda}{\rho c} t_0}$	length scale
ρ	mass density
c	heat capacity per unit mass
λ	heat conductivity
Δu_{in}	uniform intial undercooling
L	latent heat
Δs	difference in entropy density
σ	surface tension
α	coefficient of attachment kinetics

Table 2. Table of real parameters.

Model parameter	Sense	Definition
L	dimensionless latent heat	$L = \frac{L_{real}}{\rho c \Delta u_{in}}$
α	kinetic coefficient	$\alpha = \alpha_{real} \frac{\lambda}{\rho c}$
β	physical parameter	$\beta = \frac{\Delta s}{\sigma} L_0 \Delta u_{in}$
ξ	interface-thickness scale	$\xi = \frac{\xi}{L_0}$
L_1, L_2	domain size	$L_{1,2} = \frac{L_{1,2,real}}{L_0}$
ξt	time step	$\xi t = \frac{\xi t_{real}}{t_0}$

Table 3. Table of model parameters.

A detailed evolution of complex shapes during the time of ≈ 1.0 has been observed in case of $\xi > h_1, h_2$ and for grid dimensions $\approx 150 \times 150$ or higher. This type of simulation requires for about 1.5 hours on the Hewlett Packard 730 workstation (with vectorization). Several quantitative studies, where the parameter ξ was very small ($< 10^{-2}$), and the domain Ω too big ($\operatorname{diam} \Omega > 10$), took many times more of the CPU time, and were at the limit of power of available computers.

Qualitative properties of the model. The model is based on the system of equations

$$\frac{\partial u}{\partial t} = \nabla^2 u + L \frac{\partial p}{\partial t}, \tag{35}$$

$$\alpha \xi^2 \frac{\partial p}{\partial t} = \xi^2 \nabla^2 p + ap(1-p)(p - 0.5 + M(\xi, u, \nabla p)) + a_\chi \chi. \tag{36}$$

with initial conditions

$$u\,|_{t=0}= u_0\ , \quad p\,|_{t=0}= p_0,$$

and with boundary conditions either

$$u\,|_{\partial\Omega}= u_\Omega\ , \quad p\,|_{\partial\Omega}= p_\Omega,$$

or

$$\left.\frac{\partial u}{\partial n}\right|_{\partial\Omega} = 0\ , \quad \left.\frac{\partial p}{\partial n}\right|_{\partial\Omega} = 0,$$

where

$$M(\xi, u, \nabla p) = \xi\beta arctg(\gamma_0(1-\zeta\cos(\theta(\nabla p)-\theta_0))(u^*-u)),$$

with additional noise term $a_\chi\chi$ (χ is a random variable with the uniform distribution on $\langle 0,1\rangle$, and a_χ is the amplitude). The coefficient γ_0 controls proper scaling in the model, ζ is the anisotropy strength, θ_0 is the crystallographic orientation, $\theta(\nabla p)$ the direction of ∇p, both with respect to x^1.

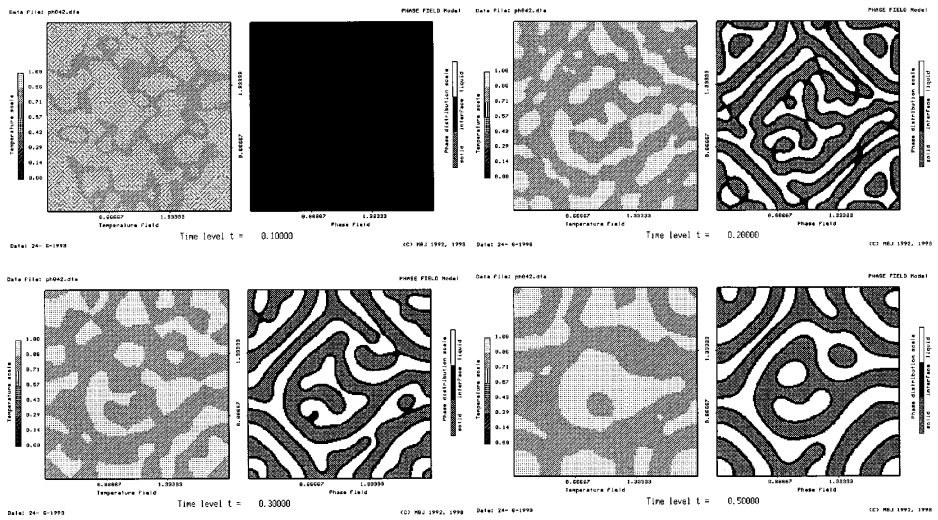

Figure 7. Spontaneous nucleation stimulated by noise, $L = 2.0$, $\beta = 900$, $\zeta = 0.2$, $\gamma_0 = 10$, $\xi = 0.01$, $\alpha = 3$, $a_\chi = 0.01$, $L_1 = L_2 = 2.0$, $\xi t = 0.1$, $N_T = 5$, $N_1 = N_2 = 100$, grid for heat equation is twice sparser.

Figure 7 shows a way the system looks for the state with minimal free energy. Noise causes a transition from the initial unstable state "1/2" to the stable states "0" and "1". The process is called spontaneous nucleation (of the solid phase). Figures 8 and 9 illustrate the single-pattern growth with dendritic structure (the interface is unstable, side-branching and competitional growth occur). The long-term behaviour is studied in Figure 14, where the surface tension causes the pattern asymptotically adopts the Wulf shape according to the form of surface energy. Directional growth where the Dirichlet boundary condition is at the left edge of the domain is in Figure 10. The planar phase interface has been modified by

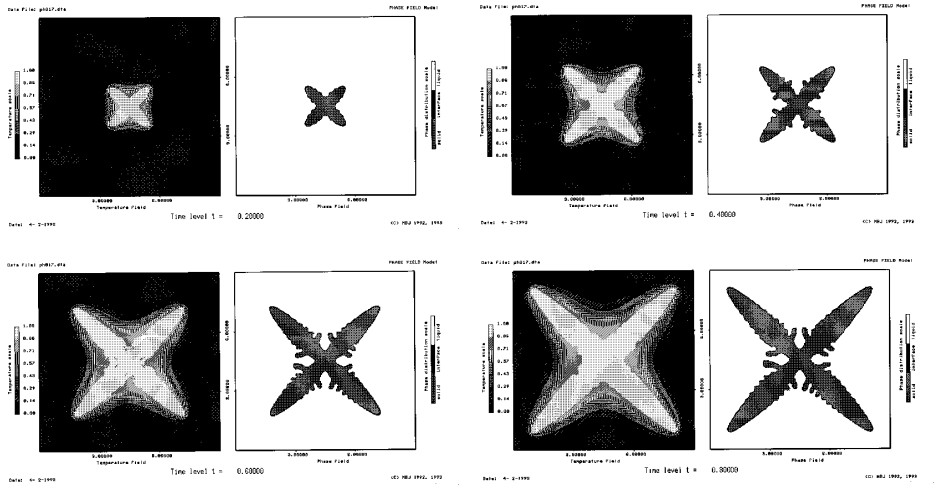

Figure 8. Growth of dendritic pattern with 4-fold anisotropy ($\zeta = 0.2$, $\gamma_0 = 10$, $\theta_0 = \frac{\pi}{4}$), $L = 2.0$, $\beta = 900$, $\xi = 0.01$, $\alpha = 3$, $a_\chi = 0.01$, $L_1 = L_2 = 9.0$, $\xi t = 0.2$, $N_T = 5$, $N_1 = N_2 = 290$.

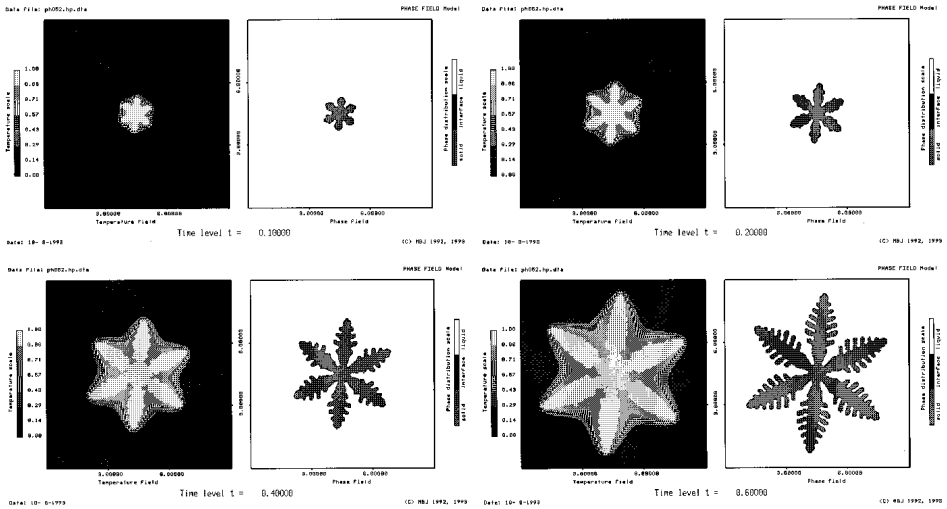

Figure 9. Growth of dendritic pattern with 6-fold anisotropy ($\zeta = 0.6$, $\gamma_0 = 10$, $\theta_0 = -0.1$), $L = 2.0$, $\beta = 900$, $\xi = 0.01$, $\alpha = 3$, $a_\chi = 0.01$, $L_1 = L_2 = 9.0$, $\xi t = 0.1$, $N_T = 10$, $N_1 = N_2 = 300$.

a sinusoidal perturbation causing evolution of a dendritic structure. Figure 11 demonstrates a competitional growth of uniformly orientated patterns. Dendrites interact by the temperature field in their neighborhood. The growth is stopped if the temperature gradient tends to 0 near a dendrite tip (overlap of thermal layers).

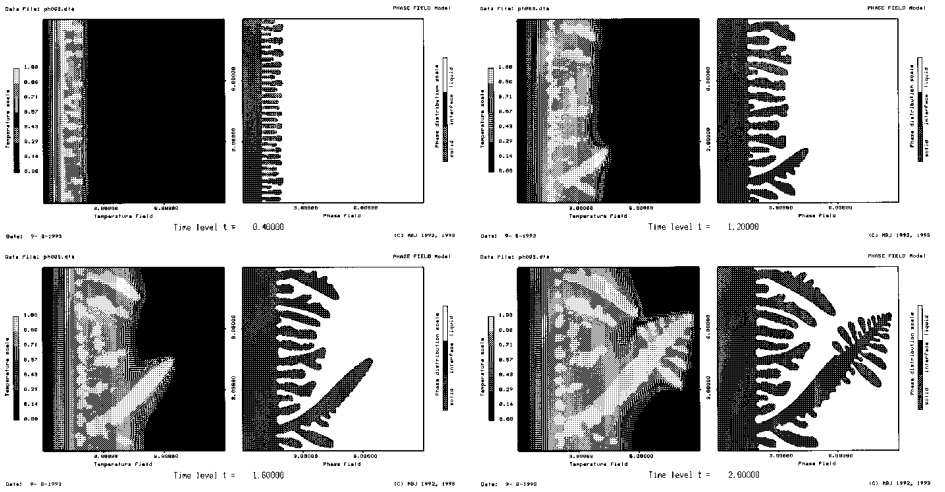

Figure 10. Directional growth with unstable phase boundary, 4-fold anisotropy, ($\zeta = 0.2$, $\gamma_0 = 10$, $\theta_0 = \frac{\pi}{4}$), $L = 2.0$, $\beta = 900$, $\xi = 0.01$, $\alpha = 3$, $a_\chi = 0.01$, $L_1 = L_2 = 9.0$, $\xi t = 0.4$, $N_T = 5$, $N_1 = N_2 = 150$, grid for heat equation is twice sparser.

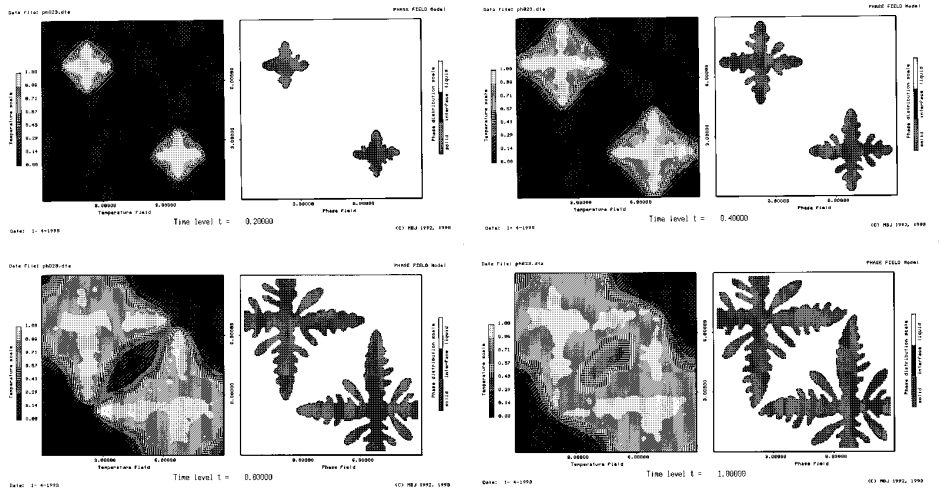

Figure 11. Competitional growth of dendritic patterns with 4-fold anisotropy ($\zeta = 0.15$, $\gamma_0 = 10$), $L = 2.0$, $\beta = 900$, $\xi = 0.01$, $\alpha = 3$, $a_\chi = 0.01$, $L_1 = L_2 = 9.0$, $\xi t = 0.2$, $N_T = 5$, $N_1 = N_2 = 200$.

The crystalline orientation is an individual property of any pattern which has begun growing by nucleation. To improve the phase field model, an other intensive variable depending on time and space has been introduced in [**3**]. The function $\theta = \theta(x,t) \in \{0\} \cup (\pi, 3\pi\rangle$ describes the orientation distribution in Ω. The value 0

represents the trivial non-activated state of an arbitrary point $x \in \Omega$ at $t \in \langle 0, T\rangle$, if no orientation is joint with this point. Other values correspond to the relative angle between the crystal orientation and the x^1 axis. The function θ has to be activated everywhere on $\Omega_s(0)$ and $\Omega_\Gamma(0)$ at the beginning of the simulation. The evolution of the function θ is simultaneous with the evolution of the phase function where a simple explicit rule defines updated values of θ on the grid:

$$\theta_{ij}(t+\xi t) = \max\{\theta_{kl}(t) \mid k = i-1, i, i+1 \wedge l = j-1, j, j+1\}.\Theta(p(t)_{ij} - p_{\text{crit}}), \tag{37}$$

where ξt is the actual time step of the Runge-Kutta method, $\Theta(p)$ is the step function:

$$\Theta(p) = 0 \quad \text{if } p < 0\ , \quad \Theta(p) = 1 \quad \text{if } p > 0,$$

where i, j are the x^1 and x^2 indices of the nodes in the grid, p_{crit} is a critical value of the variable p defining the up-dating of the orientation function (it has been chosen $p_{\text{crit}} = 0.05$ in presented computational results). Using the formula (37), the orientation of dendrites is non-trivial in $\Omega_s(t)$ and $\Omega_\Gamma(t)$ only and is supported by the phase function p. This fact allows to separate orientations of different growing shapes if they are represented by disjoint continuous subsets of $\Omega_s(t)$. Results of simulation using the improved model with the orientation separation are in Figure 12.

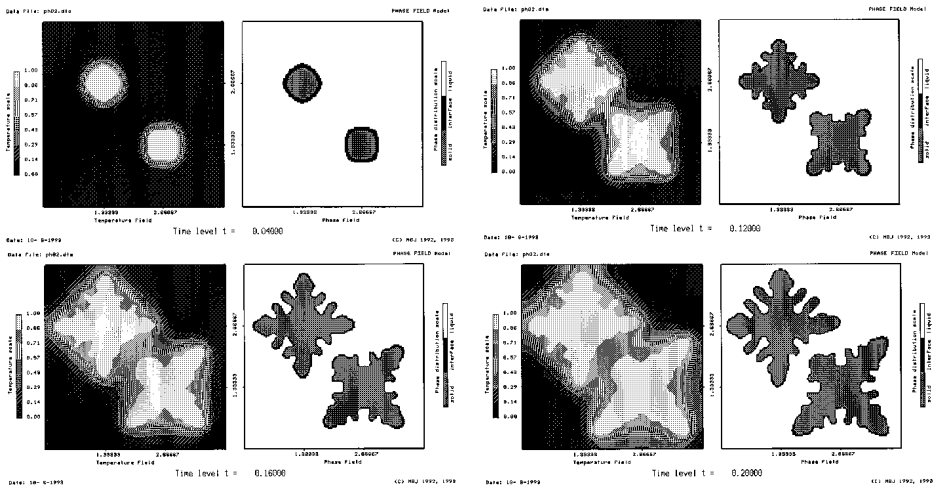

Figure 12. Competitional growth of dendritic patterns with 4-fold anisotropy and different crystalline orientation ($\zeta = 0.2$, $\gamma_0 = 10$, $\theta_1 = 0.0$, $\theta_2 = \frac{\pi}{4}$), $L = 2.0$, $\beta = 900$, $\xi = 0.01$, $\alpha = 3$, $a_\chi = 0.01$, $L_1 = L_2 = 4.0$, $\xi t = 0.04$, $N_T = 10$, $N_1 = N_2 = 150$.

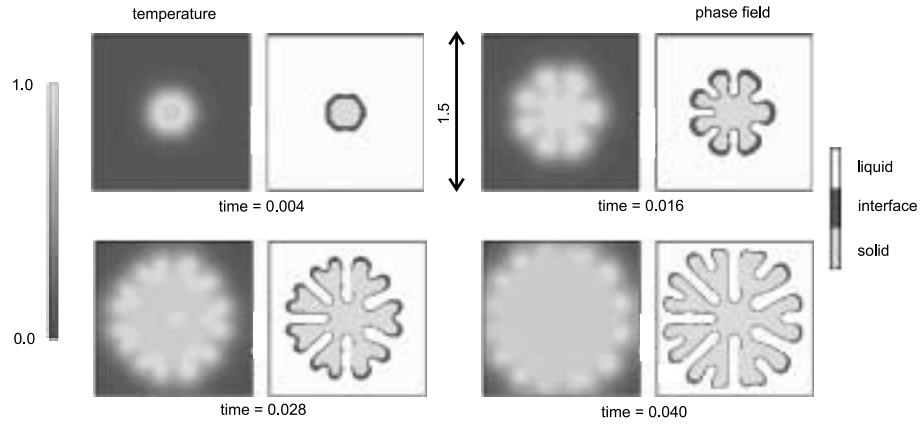

Figure 13. Isotropic dendritic growth, $L = 2.0$, $\beta = 900$, $\zeta = 0.0$, $\xi = 0.01$, $\alpha = 3$, $a = 2.0$, $L_1 = L_2 = 1.5$, $\xi t = 0.004$, $N_T = 10$, $N_1 = N_2 = 150$.

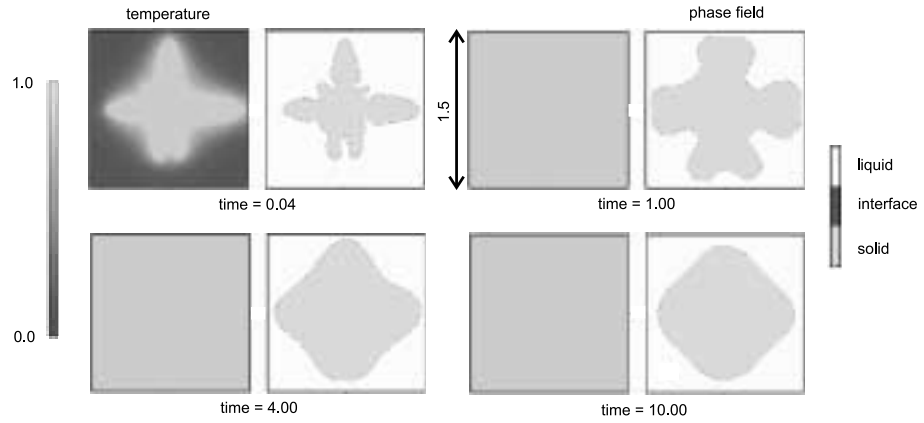

Figure 14. Coarsening – longterm behaviour of the pattern with 4-fold anisotropy, $L = 2.0$, $\beta = 900$, $\zeta = 0.5$, $\xi = 0.005$, $\alpha = 3$, $a = 4.0$, $L_1 = L_2 = 1.5$, $\xi t = 1.0$, $N_T = 10$, $N_1 = N_2 = 200$.

Quantitative analysis. As shown by detailed numerical studies [**3**], [**6**], [**7**], a quantitatively correct anisotropic model has to be set as follows:

$$\frac{\partial u}{\partial t} = \nabla^2 u + L\frac{\partial p}{\partial t}, \tag{38}$$

$$\alpha\xi^2\frac{\partial p}{\partial t} = g(\theta)[\xi^2\nabla^2 p + ap(1-p)(p-0.5)] + \beta F(u)\xi^2|\nabla p|_E, \tag{39}$$

with initial conditions

$$u\,|_{t=0} = u_0\ , \quad p\,|_{t=0} = p_0,$$

and with boundary conditions either

$$u\,|_{\partial\Omega} = u_\Omega\ , \quad p\,|_{\partial\Omega} = p_\Omega,$$

or

$$\left.\frac{\partial u}{\partial n}\right|_{\partial\Omega} = 0\ , \quad \left.\frac{\partial p}{\partial n}\right|_{\partial\Omega} = 0,$$

where g is the function describing anisotropy:

$$g(\theta) = 1 - \zeta\cos(\theta - \theta_0)n_{\text{fold}}$$

with $\zeta \in \langle 0, 1)$ being the n_{fold}-anisotropy strength, θ the direction of ∇p, and θ_0 principal crystallographic orientation, both relative to $\mathbf{x}_1$. The coupling function has the form $F(u) = \min\{10, \max\{-10, u^* - u\}\}$ with u^* being the melting point.

We present a study investigating a quantitative relationship to the sharp-interface standard such as an analytical solution or a previously known criterion. Stability of planar interface is investigated in order to analyse the interaction of curvature and undercooling (see [**5**]). A sinusoidal perturbation is used to demonstrate stability of such a front. Let the direction of the front motion coincide with the direction of $\mathbf{x}_1$, and let the perturbation have the following form:

$$x^1 = \epsilon\sin\omega x^2 \quad .$$

Mean curvature of such perturbed interface is

$$\kappa_\Gamma = -\frac{\frac{d^2x^1}{d(x^2)^2}}{(1 + (\frac{dx^1}{dx^2})^2)^{\frac{3}{2}}},$$

where

$$\frac{dx^1}{dx^2} = \epsilon\omega\cos\omega x^2,$$
$$\frac{d^2x^1}{d(x^2)^2} = -\epsilon\omega^2\sin\omega x^2.$$

Therefore, up to the first order in powers of ϵ, if this is small, the maximal and minimal values of curvature along the interface are:

$$\kappa_- \approx -\epsilon\omega^2,$$
$$\kappa_+ \approx \epsilon\omega^2,$$

Assume that corresponding temperature and velocity of the interface are

$$u_- = u_{-\infty}, \qquad u_+ = u_{-\infty} + G\epsilon,$$

where u_- is temperature far behind the front, and

$$G = -L\frac{\Delta s}{\alpha\sigma\lambda}\,(u^* - u_{-\infty})\,.$$

Obviously, a front instability occurs if $v_{\Gamma_+} - v_{\Gamma_-} > 0$.

The condition (27) being valid at the interface Γ yields the following instability conditions

$$\omega^2 + \frac{\xi s}{2\sigma}G < 0, \ \text{ if } \quad \epsilon < \frac{L}{\rho c \mid G \mid},$$
$$2\epsilon\omega^2 - \frac{\Delta s L}{\sigma\rho c} < 0, \ \text{ if } \quad \epsilon \geq \frac{L}{\rho c \mid G \mid},$$

which differ by the relation of temperature gradient at the interface and the amplitude of perturbation. Such conditions have been used to set up the system parameters in order to get stable and unstable behaviour of the planar front. As shown in Figure 15 and 16, the phase field solution exhibits corresponding stability behaviour. Note that the above derived stability criterion is in agreement with the Mullins-Sekerka stability analysis [**31**], [**32**]. The above presented analysis does not consider the case of dendritic growth from a spherical site.

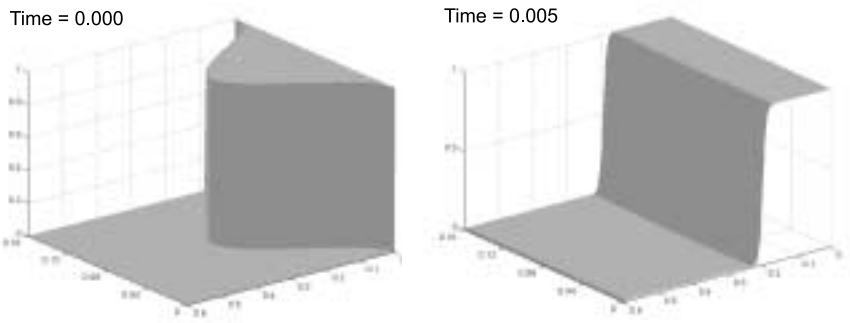

Figure 15. Stability of the two-dimensional travelling-wave solution of equations for $\xi = 0.005$. Other parameters are $u(0) = -1.05$, $u_{left} = 0.95$, $u_{right} = -0.05$, $L = 1.0$, $\beta = 10$, $a = 2.0$, $D_0 = \lambda/\rho c = 1.0$, $\alpha = 1$, $L_1 = 0.6$, $L_2 = 0.16$, $\xi t = 0.001$, $N_T = 5$, $N_1 = 400$, $N_2 = 100$. The figure shows the profile of p at $t = 0.0$ and $t = 0.005$.

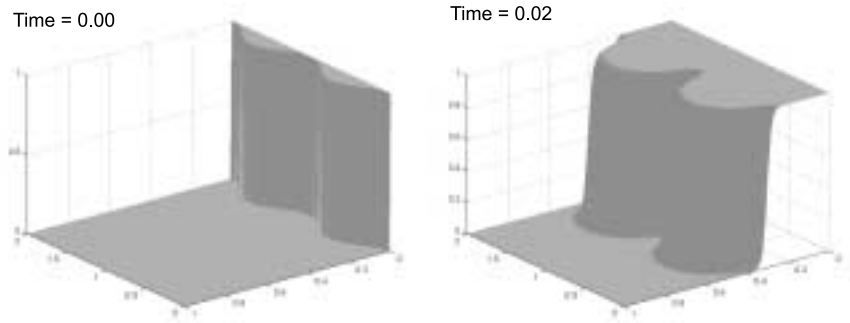

Figure 16. Instability of the two-dimensional travelling-wave solution of equations for $\xi = 0.01$. Other parameters are $u(0) = -5.5$, $u_{top} = 0.5$, $u_{bottom} = -5.5$, $L = 6.0$, $\beta = 10$, $a = 2.0$, $D_0 = \lambda/\rho c = 1.0$, $\alpha = 1$, $L_1 = 1.0$, $L_2 = 2.0$, $\xi t = 0.004$, $N_T = 5$, $N_1 = 200$, $N_2 = 400$. The figure shows the profile of p at $t = 0.0$ and $t = 0.02$.

9. Conclusion

The article was devoted to presenting the actual state of the art of mathematical modelling of microstructure growth in solidification with focus on pure substances

and on a diffuse-interface approach to it. Tha main problem still remains to solve — to get a quantitatively good model which realiably simulate formation of dendritic or just geometrically complex structures. An appropriate combination of various techniques together with increasing efficiency of supercomputing tools may represent a way towards a progress in this field.

Acknowledgment. The work of the author in the area covered by this article has been partly supported by the projects MSM J98/210000010 and MSM J98/242200001 of the Czech Ministry of Education, and also by the project Barrande 2001-036-1 of the French-Czech Cooperation Programme.

References

1. Almgren R., *Variational algorithms and pattern formation in dendritic solidification*, J. Comput. Phys. **106** (1993), 337–354.
2. Beneš M., *Finite difference numerical solution of the two-dimensional Stefan problem*, Acta Polytechn. CVUT **18**(IV,1) (1989), 61–87.
3. ———, *Computational studies of the dendritic crystal growth in pure materials*, Technical report, Laboratoire de Métallurgie Physique, École Polytechnique Fédérale de Lausanne, 1993.
4. ———, *Modelling of dendritic growth in pure substances*, Acta Techn. CSAV **39** (1994), 375–397.
5. ———, *On a computational comparison of phase-field and sharp-interface model of microstructure growth in solidification*, Acta Techn. CSAV **41** (1996), 597–608.
6. ———, *Phase-Field Model of Microstructure Growth in Solidification of Pure Substances*, PhD thesis, Faculty of Nuclear Sciences and Physical Engineering, Czech Technical University, 1997.
7. ———, *Numerical simulation of microstructure growth in solidification by the phase-field model with a gradient coupling term*, In ACOMEN'98, Advanced Computational Methods in Engineering (R. Van Keer, R. Verhegghe, M. Hogge, and E. Noldus, eds.), pages 343–350, Maastricht, 1998.
8. ———, *Anisotropic phase-field model with focused latent-heat release*, In FREE BOUNDARY PROBLEMS: Theory and Applications II, pages 18–30, Chiba, Japan, 2000, GAKUTO International Series Mathematical Sciences and Applications, Vol. **14**.
9. ———, *Numerical solution of phase-field equations with a gradient coupling term*, In Partial Differential Equations – Theory and Numerical Solution (W. Jäger, J. Nečas, O. John, K. Najzar and J. Stará, eds.), pages 25–33, New York, 2000.
10. ———, *Mathematical analysis of phase-field equations with numerically efficient coupling terms*, Interfaces and Free Boundaries **3** (2001), 201–221.
11. Beneš M., Krejčí L., Vogel J., Kerner J. and Šára L., *Heat conduction in a steel plate- or cylindric casting. Technical report*, Research Report of the Czechoslovak Academy of Sciences, Institute of Thermomechanics, 1990 (in Czech).
12. Beneš M. and Mikula K., *Simulation of anisotropic motion by mean curvature–comparison of phase-field and sharp-interface approaches*, Acta Math. Univ. Comenianae **67**(1) (1998), 17–42.
13. Bonacina C. and Comini G., *Numerical solution of phase-change problems*, Int. J. Heat Mass Transfer **16** (1973), 1825–1832.
14. Bronsard L. and Kohn R., *Motion by mean curvature as the singular limit of Ginzburg-Landau dynamics*, J. Differential Equations **90** (1991), 211–237.
15. Brown S. G. R., Williams T. and Spittle J. A., *A cellular automaton model of the steady-state 'free' growth of a non-isothermal dendrite*, Acta metall. mater. **42** (1994), 2893–2898.

16. Caginalp G., *An analysis of a phase field model of a free boundary*, Arch. Rational Mech. Anal. **92** (1986), 205–245.
17. Cahn J. W. and Hilliard J. E., *Free energy of a nonuniform system. I. Interfacial free energy*, J. Chem. Phys. **28** (1958), 258–267.
18. ———, *Free energy of a nonuniform system. III. nucleation of a two-component incompressible fluid*, J. Chem. Phys. **31** (1959), 688–699.
19. Chalmers B., *Principles of Solidification*, R. E. Krieger Publishing, Huntington, New York, 1977.
20. Crandall M. G., Ishii H. and Lions P.-L., *User's guide to viscosity solutions of second-order partial differential equations*, Bul. AMS **27** (1992), 1–67.
21. Dziuk G., *Algorithm for evolutionary surfaces*, Numer. Math. **58** (1991), 603–611.
22. Eckmann J. P., Meakin P., Procaccia I. and Zeitak R., *Growth and form of noise-reduced diffusion-limited aggregation*, Phys. Rev. A **39** (1989), 3189–3195.
23. Gaponov-Grekhov A. V. and Rabinovich M. I., *Disorder, dynamical chaos and structures*, Physics Today, July 1990, 30–38.
24. Gurtin M., *On the two-phase Stefan problem with interfacial energy and entropy*, Arch. Rational Mech. Anal. **96** (1986), 200–240.
25. Hohenberg P. C. and Halperin B. I., *Theory of dynamic critical phenomena*, Rev. Mod. Phys. **49** (1977), 435–479.
26. Kessler D. A., Koplik J. and Levine H., *Geometrical models of interface evolution. III. Theory of dendritic growth*, Phys. Rev. A **31** (1985), 1712–1717.
27. Kobayashi R., *Modeling and numerical simulations of dendritic crystal growth*, Physica D **63** (1993), 410–423.
28. Kurz W. and Fischer D. J., *Fundamentals of Solidification*, Trans. Tech. Publishers, Aedermannsdorf, 1989.
29. Langer J. S., *Instabilities and pattern formation in crystal growth*, Reviews of Modern Physics **52** (1980), 1–28.
30. Meyer G. H., *Multidimensional Stefan problems*, J. Numer.Anal. **10** (1973), 522–538.
31. Mullins W. W. and Sekerka R. F., *Morphological stability of a particle growing by diffusion or heat flow*, J. Appl. Phys. **34** (1963), 323–329.
32. ———, *Stability of a planar interface during solidification of a dilute binary alloy*, J. Appl. Phys. **35** (1964), 444–451.
33. Nicolis G. and Prigogin I., *Self-Organisation in Nonequilibrium Systems*, Wiley and Sons, New York, 1977.
34. Penrose O. and Fife P. C., *Thermodynamically consistent models of phase-field type for the kinetics of phase transitions*, Physica D **43** (1990), 44–62.
35. Rappaz M., *Solidification process: Constitutive equations and microstructures*, In Mathematical Modelling of Material Processing (M. Cross, J. F. T. Pittman, and R. D. Wood, eds.), pages 67–91, Oxford, 1993.
36. Rowlinson J. S., *Translation of J.D. van der Waals' 'The thermodynamic theory of capillarity under the hypothesis of a continuous variation of density'*, J. Stat. Phys. **20** (1979), 197–244.
37. Saito Y., Goldbeck-Wood G. and Müller-Krumbhaar H., *Dendritic crystallization: Numerical study of the one-sided model*, Phys. Rev. Lett. **58** (1987), 1541–1543.
38. Schmidt A., *Die Berechnung dreidimensionaler Dendriten mit Finiten Elementen*, PhD thesis, Universität Freiburg, 1993.
39. Sethian J. A., *Level Set Methods*, Cambridge University Press, New York, 1996.
40. Smoller J., *Shock Waves and Reaction-Diffusion Equations*, Springer Verlag, Berlin, 1993.
41. Tarzia D. A., *A bibliography on moving-free boundary problems for the heat-diffusion equation. the Stefan and related problems*, MAT, Serie A **2** (2000), 1–300.
42. Vabishchevich P. N., *Numerical Methods for Solution of Free Boundary Problems*, Moscow University Press, Moscow, 1987.
43. Visintin A., *Models of Phase Transitions*, Birkhäuser, Boston, 1996.

44. Wang S.-L., Sekerka R. F., Wheeler A. A., Murray B. T., Coriell S. R., Braun R. J. and McFadden G. B., *Thermodynamically consistent phase-field models for solidification*, Technical Report 4956, NIST, U.S. Dept. of Commerce, 1992.

45. Xiao R. F., Alexander J. I. D. and Rosenberger F., *Morphological evolution of growing crystals: A Monte Carlo simulation*, Phys. Rev. A **38** (1988), 2447–2456.

M. Beneš, Department of Mathematics, Faculty of Nuclear Sciences and Physical Engineering, Czech Technical University, Trojanova 13, 120 00 Prague, Czech Republic